Numerical Analysis of Two-Dimensional Nonsteady Detonations

S. Taki*
Fukui University, Fukui, Japan
and
T. Fujiwara†
Nagoya University, Nagoya, Japan

In the present work, a system of two-dimensional nonsteady hydrodynamic and chemical kinetic equations was numerically integrated for an exothermic system. An assumed two-step reaction model simulates an oxyhydrogen mixture. The calculation starts from a plane Chapman-Jouguet detonation as an initial condition. Two-dimensional disturbances are generated by artificially placing nonuniformities ahead of the detonation front. Regardless of the difference in the given initial disturbances, a fixed number of triple shock waves were produced for a fixed combination of mixture model and geometry when the transition period was over. This shows that for a given detonation tube geometry, any exothermic system has its own characteristic multidimensional structure. The obtained number of triple shock waves contained in the detonation front was in agreement with existing experimental observations under the same condition.

Introduction

THE multidimensional nonsteady structure of a self-sustaining detonation has been observed experimentally for over a decade. Studies of the detonation limit revealed that transverse shock waves behind a leading shock wave are indispensable in sustaining detonation propagation.[1] Theoretical studies on this departure from one-dimensionality and steadiness have been originated by Shchelkin.[2] He obtained an instability criterion for a plane Chapman-Jouguet detonation wave, assuming a rectangular wave profile. The instability criterion was further expanded by Erpenbeck[3] for more realistic, one-dimensional wave profiles and for several modes of instability. The analytical work of Erpenbeck was later corroborated by Fickett and Wood[4] using numerical integration of time-dependent one-dimensional hydrodynamic equations. However, little is known as yet about the instability criteria of multidimensional detonations.[5,6] The present work is intended to elucidate instability characteristics of multidimensional detonations. To do this, a system of two-dimensional nonsteady hydrodynamic and chemical kinetic equations was solved numerically. A plane steady Chapman-Jouguet detonation is used as an initial condition. Several nonuniformities are placed ahead of the detonation front to trigger two-dimensional perturbations. The calculation shows the growth of instabilities leading to transverse shock waves in a two-dimensional channel.

Mathematical Formulation

Instead of using many real elementary reactions, a two-step model reaction was utilized in the calculation[7]; the chemical reaction was split into two stages, the first induction period and the subsequent exothermic one. The rate constants were so selected as to correspond to a diluted stoichiometric oxyhydrogen mixture:

$$w_\alpha = \frac{d\alpha}{dt} = \frac{-1}{\tau_{ind}} = -k_1 \rho \exp(-E_1/RT) \tag{1}$$

$$w_\beta = \frac{d\beta}{dt} = -k_2 p^2 \left\{ \beta^2 \exp\left(\frac{-E_2}{RT}\right) - (1-\beta)^2 \times \exp\left(-\frac{E_2+q}{RT}\right) \right\} \tag{2}$$

$$\left.\begin{aligned} k_1 &= 3.0\times 10^{11}\ \text{cm}^3/\text{g/sec}, \quad R = 6.929\times 10^6\ \text{erg/g/°K} \\ E_1/R &= 9800\ \text{K}, \quad E_2/R = 2000\ \text{K}, \quad q = 4\times 10^{10}\ \text{erg/g} \end{aligned}\right\} \tag{3}$$

where p, ρ, T, and R denote the pressure, density, temperature, and gas constant, respectively. The reaction progress parameters α and β are $1>\alpha>0$ and $\beta=1$ in the induction period, $\alpha=0$ and $1>\beta>0$ in the exothermic period.

In deriving fundamental equations, the gas is assumed to be perfect, nonviscous, and non-heat-conducting. Two-dimensional nonsteady gasdynamic equations, including the above chemical reaction, become

$$\frac{\partial f}{\partial t} + \frac{\partial F}{\partial x} + \frac{\partial G}{\partial y} + \Phi = 0 \tag{4}$$

$$f = \begin{bmatrix} \rho \\ \rho u \\ \rho v \\ \rho e \\ \rho\beta \\ \rho\alpha \end{bmatrix} \qquad F = \begin{bmatrix} \rho u \\ \rho u^2 + p \\ \rho uv \\ \rho u[e + (p/\rho)] \\ \rho u\beta \\ \rho u\alpha \end{bmatrix} \tag{5}$$

$$G = \begin{bmatrix} \rho v \\ \rho vu \\ \rho v^2 + p \\ \rho v[e + (p/\rho)] \\ \rho v\beta \\ \rho v\alpha \end{bmatrix} \qquad \Phi = \begin{bmatrix} 0 \\ 0 \\ 0 \\ 0 \\ \rho w_\beta \\ \rho w_\alpha \end{bmatrix} \tag{6}$$

$$p = \rho RT \tag{7}$$

$$e = RT/(\gamma - 1) + \beta q + \tfrac{1}{2}(u^2 + v^2) \tag{8}$$

Presented as Paper 76-404 at the AIAA 9th Fluid and Plasma Dynamics Conference, San Diego, Calif., July 14-16, 1976; submitted Aug. 2, 1976; revision received Aug. 29, 1977.

Index categories: Combustion Stability; Shock Waves and Detonations; Computational Methods.

*Associate Professor, Department of Mechanical Engineering. Member AIAA.

†Associate Professor, Department of Aeronautical Engineering. Member AIAA.

where u, v, γ, and q are the velocities in the x and y directions, respectively, the specific heat ratio, and the exothermicity. These equations were reduced to dimensionless forms by using the following characteristic physical quantites: l^* is the induction reaction length of $C-J$ detonation, ρ_0 is the initial mass density; and q is the heat of reaction per unit mass.

Based on these quantities, the references for the time, the velocity, the pressure, the temperature, and the energy can be formulated as

$$\left.\begin{aligned} &t^* \sim l^*/\sqrt{q},\ v^* = \sqrt{q} \\ &p^* = \rho_0 q,\quad T^* = q/R,\quad e^* = q \end{aligned}\right\} \tag{9}$$

The rate constants k_1 and k_2 and the activation energies E_1 and E_2 are nondimensionalized as well:

$$\left.\begin{aligned} &K_1 = k_1 \rho_0 t^*,\quad K_2 = k_2 p^{*2} t^* \\ &\epsilon_1 = E_1/q,\quad \epsilon_2 = E_2/q \end{aligned}\right\} \tag{10}$$

The initial condition for the present calculation is a plane steady Chapman-Jouguet detonation propagating in an infinitely long two-dimensional channel filled with an exothermic combustible mixture. In order to generate transverse disturbances to this plane structure, density nonuniformities are placed in front of the detonation. A particular case of one pair of density spots is shown in Fig. 1. When the detonation front arrives at these spots, it starts being subjected to lateral motion by the local differences in exothermicity.

The conditions that the six independent variables indicated in Eq. (4) have to satisfy on the solid walls can be derived as follows: Since it is assumed that the flow is nonviscous and there is no mass and heat transfer between the wall and the flow, the existence of a solid boundary can be replaced by taking into account the symmetrical mirror image of the flow. Thereafter we multiply Eq. (4) with a thin slab $1 \times \Delta y$ which contains the boundary streamline symmetrically, and integrate with respect to dy over the thickness Δy. Taking into account that the thickness of the slab is extremely small, we finally obtain, as boundary conditions,

$$[G]^{1}_{-1} = 0 \tag{11}$$

where 1 and -1 designate the quantities on the upper and lower surfaces of the slab, respectively. Since the flowfield is symmetrical with respect to the boundary streamline, we can put $v_1 = -v_{-1}$, which automatically reduces the boundary conditions (11) into a simplified and well-known form

$$v_1 = v_{-1} = 0,\ \text{or}\ v = 0\ \text{on the solid wall} \tag{12}$$

Since this turned out to be the only boundary condition, any other constraints are unnecessary on the wall.

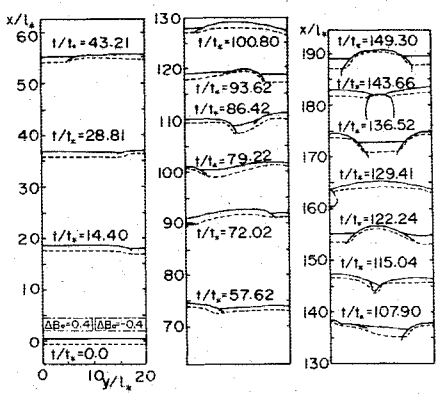

Fig. 1 History of shock front structure in a propagating detonation. Lateral distortion of the shock wave starts from the two concentration spots, shown by chain lines, located around $x/l^* = 3$ at $t/t^* = 0$. Solid curves indicate shock fronts while broken ones represent reaction fronts; $d/l^* = 20$.

However, it becomes necessary in the following numerical analysis to know other quantities on the wall. To do that, we make use of the above-mentioned mirror-image instead of the wall. In other words, we use $(A)^n_{j,1} = (A)^n_{j,-1}$ for $A = \rho, u, e, \beta$, and α, in order to obtain $(A)^n_{j,0}$, the quantity on the wall.

Numerical Analysis

The differential equation (4) can be approximated by the following first-order explicit method[8] with accuracy better than the Rusanov method:

$$f^{n+1}_{l,m} = f^n_{l,m} - (\lambda/2)[(F_{l+1} - F_{l-1})_m + (G_{m+1} - G_{m-1})_l]^n$$

$$- \Delta t \Phi^n_{l,m} + (\lambda^2/2)[(\phi_{l+\frac{1}{2}} - \phi_{l-\frac{1}{2}})_m + (\phi_{m+\frac{1}{2}} - \phi_{m-\frac{1}{2}})_l]^n \tag{13}$$

$$\phi^n_{l+\frac{1}{2},m} = (a^2)^n_{l+\frac{1}{2},m}(f^n_{l+1,m} - f^n_{l,m}) \tag{14a}$$

$$\phi^n_{l-\frac{1}{2},m} = (a^2)^n_{l-\frac{1}{2},m}(f^n_{l,m} - f^n_{l-1,m}) \tag{14b}$$

$$(a^2)^n_{l\pm\frac{1}{2},m} = \tfrac{1}{2}[(a^2)^n_{l\pm1,m} + (a^2)^n_{l,m}] \tag{14c}$$

where $\Delta x = \Delta y$ is assumed and

$$\lambda = \frac{\Delta t}{\Delta x} = \frac{\Delta t}{\Delta y} \tag{15}$$

$$a = \sqrt{\gamma RT} + \sqrt{u^2 + v^2} \tag{16}$$

and l, m, and n indicate a lattice point in the x-y-t space.

The $n+1$-th time step is determined by the stability condition, the Courant-Friedrichs-Lewy criterion, as follows:

$$\Delta t_{n+1} = 1/\max\left\{a\sqrt{\frac{1}{(\Delta x)^2} + \frac{1}{(\Delta y)^2}}\right\}_{l,m,n} \tag{17}$$

Argon or helium diluted stoichiometric oxyhydrogen at $T_0 = 288.65$ K is chosen as the test gas, the chemical properties of which are listed as follows[7]:

$$\left.\begin{aligned} &q/RT_0 = 20.0,\ \gamma = 1.4,\ E_1/q = 1.7,\ E_1/E_2 = 4.90 \\ &k_1 = 3.6 \times 10^{12}\ \text{cm}^3/\text{mole/sec},\ t^* = 0.1827/p_0\,(\text{atm})\mu\text{sec} \\ &K_1/K_2 = 20.0 \end{aligned}\right\} \tag{18}$$

$$l^* = 0.0225/p_0(\text{atm})\quad \text{cm for } 2H_2 + O_2 + 7Ar \tag{19}$$

$$l^* = 0.05/p_0(\text{atm})\quad \text{cm for } 2H_2 + O_2 + 7He \tag{20}$$

The preceding values yield the propagation Mach number of the $C-J$ detonation,

$$M_{C-J} = \left\{1 + \frac{\gamma^2 - 1}{2\gamma}\frac{q(1-\beta_{eq})}{RT_0}\right\}^{\frac{1}{2}} + \left\{\frac{\gamma^2 - 1}{2\gamma}\frac{q(1-\beta_{eq})}{RT_0}\right\}^{\frac{1}{2}} = 4.80 \tag{21}$$

or the dimensionless propagation velocity $D_{C-J}/\sqrt{q} = 1.27$, where $\beta_{eq} = 0.2315$.

Numerical calculations were performed for the following two channel widths: 1) $d = 20\ l^*$ (calculation run 6011) and 2) $d = 12\ l^*$ (calculation run 6031). In calculation 1), $20\ l^* \times 1150\ l^*$ in x-y space was covered by the integration using 9100 lattice points, with the detonation propagated by 9.5 channel widths. On the other hand, calculation 2) covered $12\ l^* \times 921\ l^*$, using 21,051 lattice points and the detonation propagated by 10 channel widths. In both cases, the axial length under

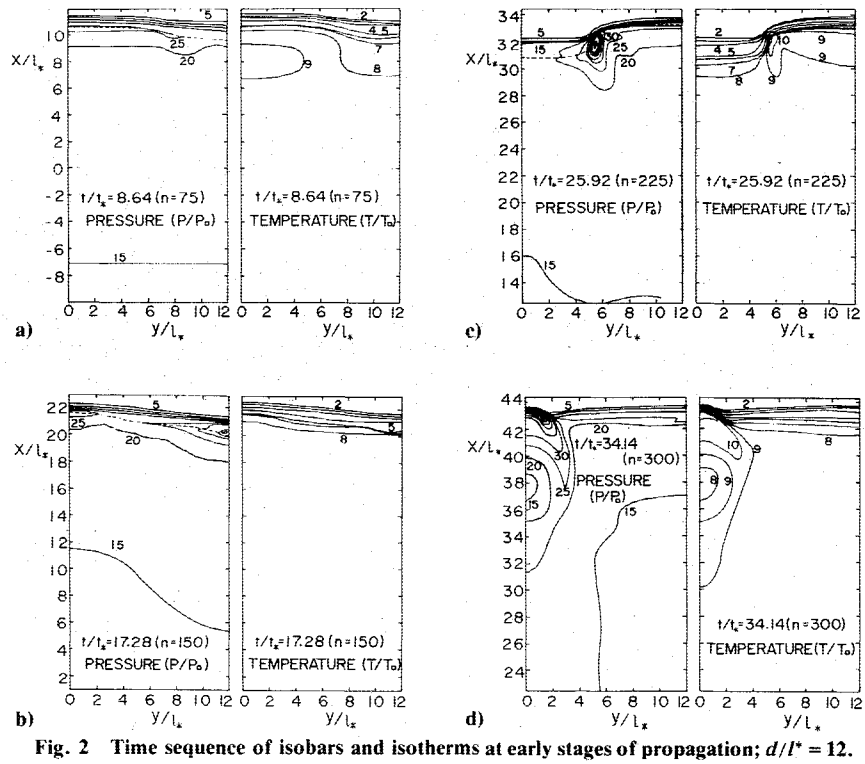

Fig. 2 Time sequence of isobars and isotherms at early stages of propagation; $d/l^* = 12$.

calculation was selected six to eight times longer than the passage of the detonation. Such sufficient length behind the detonation front made it possible for the downstream behavior of combustion products to influence the wave front; it is believed that experimentally observed triple shock waves have strong relationships with downstream phenomena.

As for the accuracy of calculation, we were concerned that the axial length covered by the calculation was insufficient, the integration step was too large, the sonic point singularity would lead to divergence, and the artificial viscosity would wipe out the presence of strong explosion waves. The former two problems were eliminated by selecting the proper axial length and step size; the selected axial length was such that any additional increase caused no change in results. Neither of the latter two problems appeared in the present calculations, mainly due to the adopted difference scheme and the step size of integration.

Results and Discussion

Development of Transverse Waves

As shown in Fig. 1, a plane and steady detonation at $t=0$ is perturbed by a pair of concentration spots placed perpendicular to the direction of wave propagation, and immediately later, as a result, there appears one concave region in the frontal structure (triple shock intersection); since this concave region moves sideways, the detonation is already two-dimensional and nonsteady. This transverse wave gradually continues to amplify up until $t/t^* = 72$, when an explosive ignition on the wall ($y=0$) generates another transverse wave. This new wave also propagates laterally and eventually collides with the original one propagating in the opposite direction at $t/t^* = 90$. From $t/t^* = 86.42$ on, the interacting feature of these two waves remains essentially unchanged, settling down into a periodical mode. At $t/t^* = 149.30$, for example, two well-developed transverse waves are interacting with each other, evidently showing reflected shock waves trailing downstream. Interestingly, after around $t/t^* = 122.24$, the calculation shows all the features that the existing experimental observations provide with phenomenological explanations for the mechanisms:

1) Collision of two triple shock waves considerably reduces the reaction time of the gas and consequently makes the reaction front approach the shock front.

2) In this sense, transverse shock waves trailing downstream always propagate to the region of longer reaction length and sweep unreacted gases.

3) After the collision of triple shocks, as seen at $t/t^* = 149.30$ for example, the front shock is accelerated by abrupt release of exothermicity; this process, shown at $t/t^* = 143.66$ and 149.30, looks more like a spherical explosion superimposed onto a plane Chapman-Jouguet detonation.

4) Collision of a triple shock with wall is identical to that between two shocks.

Figure 2 shows the history of isobars and isotherms for a narrower channel case ($d = 12l^*$). The development of the transverse wave is found to be faster compared with the case of a wider channel ($d = 20l^*$) after the passage of the same time. This triple shock wave remains alone even at the end of calculation; it means that the "eigennumber" of the triple shock is 1 for the narrower channel. The speed of the transverse wave development seems to be related to whether the number of initial perturbations is identical to the eigennumber or not; if the transverse waves initially match with the eigennumber, their development is rapid. Observing that the

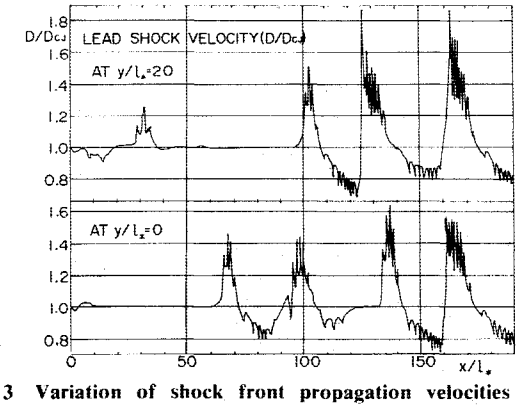

Fig. 3 Variation of shock front propagation velocities on the channel walls ($y=0$ and $y=d$); $d/l^* = 20$.

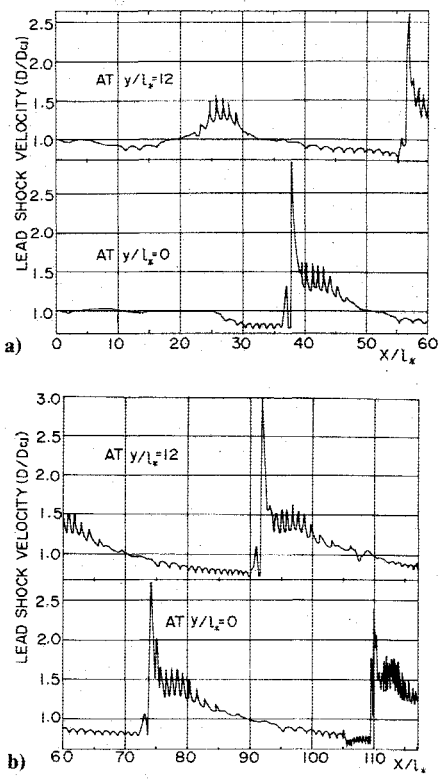

Fig. 4 Variation of shock front propagation velocities on the channel walls ($y=0$ and $y=d$); $d/l^*=12$.

formation of acoustic field downstream corresponds to the development of the transverse wave (at $t/t^*=17.28$), the interaction between the downstream acoustic wave and the frontal transverse wave results in their synchronization and cooperation to support self-sustaining detonations. In fact, this also happens in the wider channel (see Fig. 1); as soon as the number of triple shocks has increased from 1 to 2 ($t/t^*=100.80$), the acceleration of the flowfield toward a periodical structure is observed.

Spacing of Triple Shock Waves

Assuming that the number of triple shock waves appearing at the end of calculations has reached equilibrium (2 for the $20l^*$ channel, one for the $12l^*$ channel), we obtain the stationary spacing of triple shock waves, $10\sim12\ l^*$. Using Eqs. (19) and (20), a 70% argon-diluted stoichiometric oxyhydrogen gives the spacing $(0.225\sim0.27)/p_0$ cm and a 70% helium-diluted stoichiometric oxyhydrogen gives $(0.5\sim0.6)/p_0$ cm, where p_0 denotes the initial pressure in atmospheres. These values are in good agreement with existing experimental ones; $(0.27\sim0.4)/p_0$ cm for the former mixture and $(0.6\sim1.0)/p_0$ cm for the latter, obtained by Strehlow et al.[9]

Axial Propagation Velocity

The behavior of the detonation velocity in the axial direction is shown in Figs. 3 and 4. Starting from $D=D_{C-J}$, in general, the axial propagation velocity begins to fluctuate and amplify in the initial period of propagation on both walls ($y=0$ and $y=d$). Increase of the amplitude ends at $x/l^*=120$

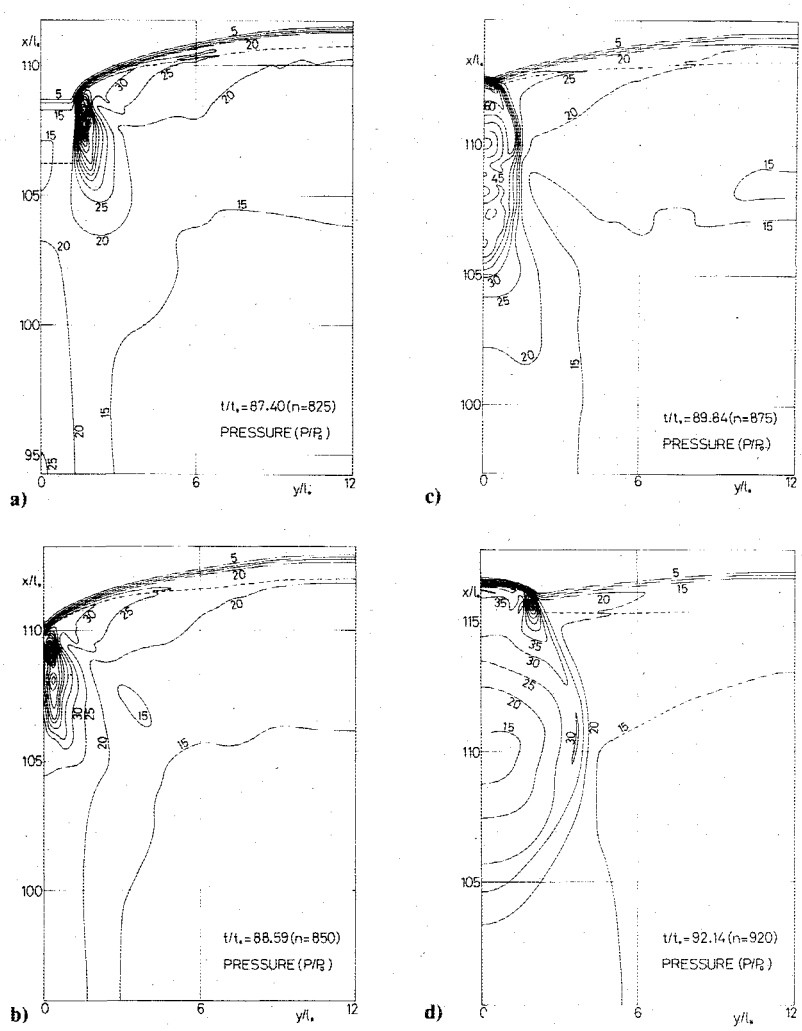

Fig. 5 Collision of a triple shock with a channel wall; a) before collision; b) collision; c) and d) after collision; $g/l^*=12$.

for the $d=20\ l^*$ channel and $x/l^*=38$ for the $d=12\ l^*$ channel, and thereafter systematic periodical patterns prevail. The significant difference in the above "pre-run" distances is conceivably caused by the eigencharacter of initial triggering of the perturbation, as mentioned previously. Note, additionally, that even if up to 60~80% velocity fluctuations are periodically observed, the average remains at $D=D_{C-J}$, which again is consistent with the existing experimental observations.

Collision of Triple Shock

Figure 5 provides the details of triple shock collision with wall. These panels a-d are more like high-precision snapshots taken during a very short time between before and after the collision. Since, in this narrower channel, transient propagation is over at $t/t^*=38$, the sequence of the collision at $t/t^*\sim 88$ is considered as a typical one. Figure 5a illustrates a snapshot before collision, where a triple shock is moving to $y=0$. The thick unburnt gas layer in front of the transverse shock indicates that this compressed and unburnt gas explodes and generates elliptic blast waves the longer axes of which are parallel to the wall. At the instant of collision, shown in Fig. 5b, two stems of the triple shock have disappeared. They re-emerge in Figs. 5c and d, where, however, the previous weak front shock has become strongest by the collision. Such a sequence resembles the collision of inert triple shock waves.[10]

Conclusions

The present numerical integration of two-dimensional nonsteady hydrodynamic equations for exothermic reactive system reproduced almost all the phenomena that existing experiments had observed, such as triple shock waves and their mutual interactions, collision of triple shocks with a wall, variation of induction distance behind front shock waves, pulsation of axial detonation velocity, Chapman-Jouguet velocity as an average, etc. Therefore, it has been confirmed that a complicated phenomenon like a detonation is simply a hydrodynamic one with high nonlinearity.

The number of triple shock waves propagating in channels is also in good agreement with existing experiments.

References

[1] Soloukhin, R. I., *Shock Waves and Detonations in Gases*, Mono Book Corp., Baltimore, 1966, pp. 138-162.

[2] Shchelkin, K. I., "Two Cases of Unstable Combustion," *Zhurnal Eksperimental'noi i Teoreticheskoi Fiziki*, Vol. 36, 1959, pp. 600-606.

[3] Erpenbeck, J. J., "Theory of Detonation Stability," *12th Symposium on Combustion*, Combustion Institute, Pittsburgh, 1969, pp. 711-721.

[4] Fickett, W. and Wood, W. W., "Flow Calculation for Pulsating One-Dimensional Detonations," *The Physics of Fluids*, Vol. 9, May 1966, pp. 903-916.

[5] Taki, S., "Nonsteady Aspects of Gaseous Detonations," Ph.D. Thesis, Nagoya University, Dept. of Aeronautical Engineering, 1974, pp. 71-114.

[6] Levin, V. A. and Markov, V. V., "Onset of a Detonation at a Concentrated Energy Deposition," *Fizika Goreniya i Vzryva*, Vol. 11, 1975, pp. 623-633.

[7] Korobeinikov, V. P., Levin, V. A., Markov, V. V. and Chernyi, G. G., "Propagation of Blast Wave in a Combustible Gas," *Astronautica Acta*, Vol. 17, Oct. 1972, pp. 529-537.

[8] Van Leer, B., "Stabilization of Difference Schemes for the Equations of Inviscid Incompressible Flow by Artificial Diffusion," *Journal of Computational Physics*, Vol. 3, 1969, pp. 473-485.

[9] Strehlow, R. A., Adamczyk, A. A., and Stiles, R. J., "Transient Studies of Detonation Waves," *Astronautica Acta*, Vol. 17, Oct. 1972, pp. 509-527.

[10] Subbotin, V. A., "Collision of Transverse Detonation Waves in Gases," *Fizika Goreniya i Vzryva*, Vol. 11, May-June 1975, pp. 486-494.